Microstructure and Wear of SLM Materials

S. Kumar [1]

Dept. of Mechanical & Aerospace Engineering, Utah State University, Logan, Utah

Reviewed, accepted September 10, 2008

Abstract

Selective Laser Melting (SLM) is increasingly used for low volume manufacturing of metallic materials. The present investigation deals with the microstructure of SLM materials (stainless steel, tool steel, Ti-6Al-4V, Co-Cr-Mo) and tries to find out the influence of processing parameters on their microstructures. Besides, fretting wear tests have been performed on them and their wear resistances have been compared with SLS materials (LaserForm, DirectSteel) and conventionally produced tool steel. It has been found that (1) porosity is still a problem for SLM materials and there exists a direct relation between processing and microstructures, (2) wear resistance of SLM/SLS materials is better than that of tool steel.

Key words: : Selective Laser Melting/Sintering (SLM/SLS), Fretting wear, Microstructure

1 Introduction

Selective Laser Sintering (SLS) is one of the most-researched rapid prototyping/manufacturing/tooling process. One of its variant, Selective Laser Melting (SLM) which relies on complete melting of materials instead of partial melting (as in case of SLS) is fast gaining ground for rapid manufacturing/tooling applications. A major component of the development for both variants is production of process-oriented powders. The development of powders for SLS is somewhat difficult as it requires engineering/design of the powder which should furnish full density by partial melting and/or infiltration. Various SLS customized powders are: LaserForm, DirectSteel, RapidSteel, DuraForm, ProtoForm, CastForm, SandForm, Fine Nylon, Copper Polyamide, Somos, etc [1].

[1] Dr. Sanjay Kumar, Mechanical & Aerospace Engineering Department, Utah State University, 4130-Old Main Hill, Logan, Utah-843222, USA, Tel: +1 435 797 1803, Fax: +1 435 797 2417, Email: sanjay.kumar@usu.edu

15 August 2008

Sl. No.	Materials Name	Trade Name	Source	SLM Machine
1	Concept Stainless Steel	CL20ES	CL GmbH	KUL
2	Concept Tool Steel	CL50WS	CL GmbH	CL
3	EOS Stainless Steel	17-4	EOS GmbH	CL
4	Ti-6Al-4V	CL 40Ti	CL GmbH	CL
5	Co-Cr-Mo	-	MTM	CL

Table 1
Materials and Machines used for SLM

Effort has also been made to develop SLS powders outside commercial companies [2–4].

For SLM, the production of customized powders is done by various SLM machine-providers. These powders are optimized for a particular SLM machine and this limits their applicability. Most of the powders are metallic-based powders such as stainless steel, tool steel, Ti-6Al-4V, Co-Cr etc [5]. There has also been research on SLM of SLS powders but it has not always given full density necessitating the need to produce dedicated powders for SLM [6].

The present research is concerned mainly with (1) the analysis of SLM steel materials produced by SLM machines, and (2) the fretting wear behaviour of SLM materials and their comparison with other materials.

2 Experiments

2.1 SLM Materials and Processing

Powders used are summarized in Table 1: (1) Stainless steel obtained from Concept Laser (CL) GmbH henceforth named as Concept stainless steel was processed on the KUL SLM machine, while (2) tool steel obtained from CL GmbH named as Concept tool steel, (3) stainless steel obtained from EOS GmbH named as EOS stainless steel, (4) Ti-6Al-4V obtained from CL GmbH and (5) locally made Co-Cr-Mo were processed on the Concept Laser (CL) Machine.

All these powders have been used already to make functional products for RM or RT (see Figure 1). Samples cut out from some of these parts were used for wear testing. Details of the powders and processing parameters are given in coming sections.

Fig. 1. RM/RT products made from Concept stainless steel, Concept tool steel, EOS stainless steel and Ti-6Al-4V respectively [7]

2.1.1 Concept Stainless Steel

This powder is a spherical stainless steel powder of size 25-50 μm named as CL20ES supplied by Concept Laser GmbH. It is recommended for the production of acid- and corrosion-resistant parts or tool components for pre-production tools.

The powder has been processed on the KUL SLM machine using following parameters: Laser Power- 150 W, Scan Spacing- 70 μm, Scan Speed- 400 mm/s and Layer Thickness- 30 μm. The products obtained are about 97% dense and their hardness is 17 HRC which is less than the stated hardness of 20 HRC for full dense products. It infers that the experimental parameters still need to be optimized for achieving the best results.

Figure 2 shows microstructures of powder and part. Microstructure of the powder shows that most powder particles are spherical as claimed by the provider. The microstructure of the part shows dark spots and patches as regular and irregular pores respectively. The irregular pores are a matter of serious concern as they show the faulty powder deposition and/or abrupt changes in powder environment, geometry or scanning conditions requiring a bigger effort for process optimization.

Figures 3 and 4 show SEM microstructures of Concept stainless steel products taken at different magnifications which clearly illustrate the formation of

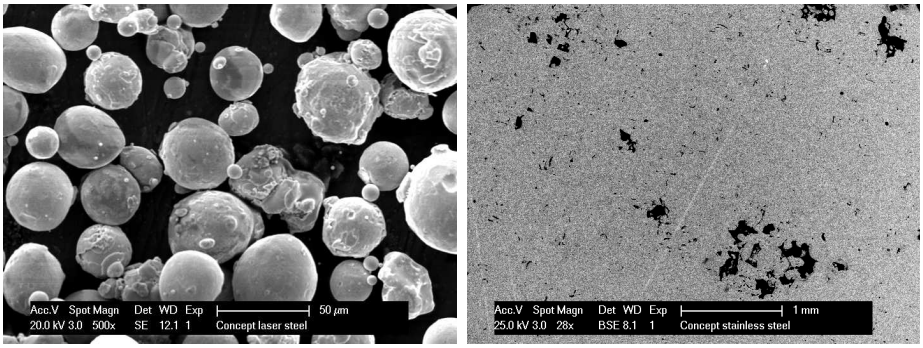

Fig. 2. Micrograph of powder and part of Concept stainless steel

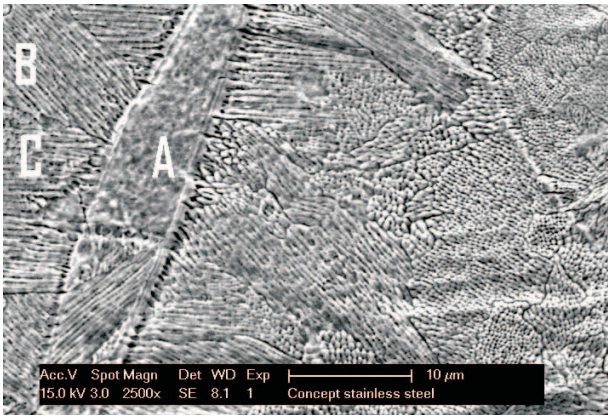

Fig. 3. Dendritic microstructures of Concept stainless steel materials

dendrites during processing. The dendrite is formed due to the creation of high thermal gradients during SLM. The prevalence of dendrites in the microstructure proves it to be the dominant mechanism for consolidation of steel-based powders in SLM.

Micrograph 3 depicts the presence of elongated as well as point-like dendrites (tip of the dendrite) showing the different direction of their growth corresponding to different direction of cooling of the melt pool. It demonstrates that the underlying layer is neither dominant nor the only source of cooling. Adjacent powder lines also act as coolant.

Broad, elongated structure (A) in the middle of the micrograph 3 shows a melt pool which makes the highest-angle grain boundaries with neighbours (grains B and C). These grain-boundaries are the area of highest mismatch and source of potential cracks or fractures. This mismatch is unavoidable but could be minimized by optimizing the process parameters (such as scan speed) during SLM which in turn will create near parallel melt pools.

Micrograph 4 illustrates the earlier described microstructure at higher magnification. Needle-like continuous dendrites are seen in the micrograph but in some areas in the middle of the grain their identities are completely lost. This

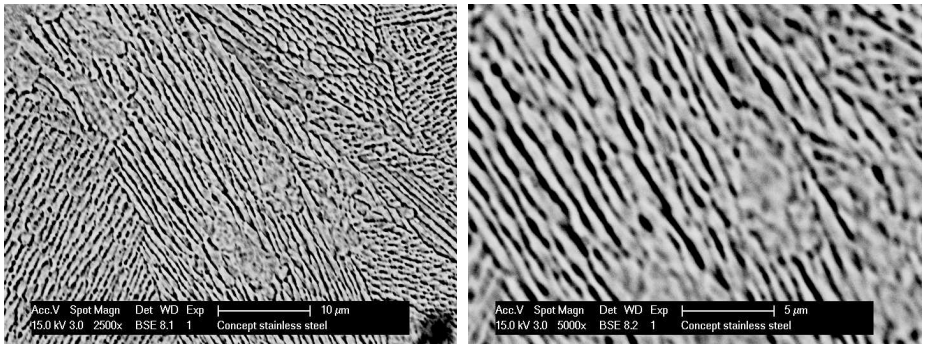

Fig. 4. Dendritic microstructures of Concept stainless steel materials at higher magnification

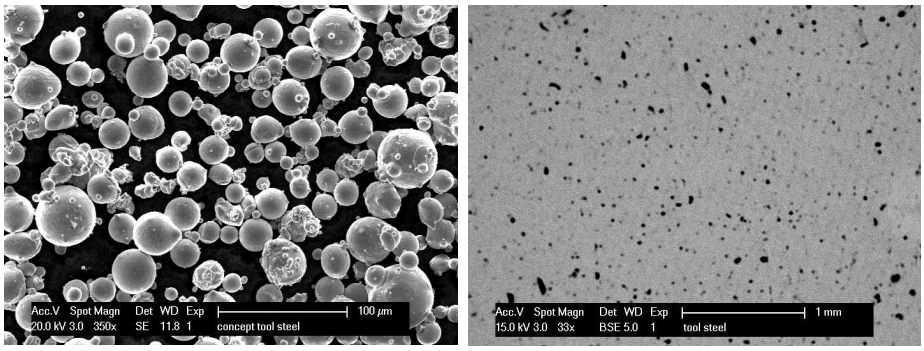

Fig. 5. Micrographs of powder and part of Concept tool steel

is due to the partial melting of underlying layer during the subsequent pass of the laser beam.

Grains are seen to have an average size of 10-15 μm which is quite large showing that there is still room for increasing the laser power which in turn will increase the thermal gradient and can decrease the grain size to 3-5 μm.

2.1.2 Concept Tool Steel

This powder is spherical powder of size 20-50 μm named CL50WS and supplied by Concept Laser GmbH. It is recommended for the production of parts with characteristics similar to hot-work steel 1.2343 as well as tool components of plastic injection moulds.

The powder has been processed in a Concept Laser machine using the following processing parameters: Laser Power- 95 W, Scanning Speed- 200 mm/s, Scan Spacing- 140 μm, Layer Thickness- 30 μm. Processing was done by using the chess board scanning strategy, that process successive square patches (islands). The processed part was about 99 % dense and hardness was 31 HRC which is less than the suggested hardness of 35-40 HRC for a fully dense part. Though the parts were processed with the recommended experimental parameters,

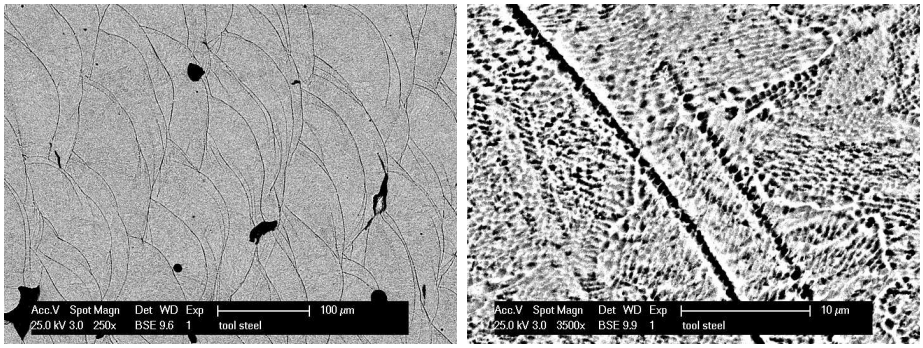

Fig. 6. Microstructure of Melt pools observed for Concept tool steel parts

they could not achieve the desired strength showing there is still a need for optimization of parameters for each individual machine.

The left side micrograph of figure 5 shows the Concept tool steel powder. It shows that the average size of the powder is about 20 μm and that the grains are mostly spherical. The right side micrograph of the figure shows the micrograph of an etched specimen taken with the help of Backscattered Scanning Electron microscopy (BSE). The micrograph comprises a number of dark black and light black points. These pores are responsible for decreasing the density of the sample. Careful observation of light dark points show that they make broken lines corresponding to the scanning lines (vectors). These could be avoided by adopting a scanning strategy which shifts the scanning lines during the formation of subsequent layers. However, for complete pore removal, other processing parameters also need to be optimized.

The left side micrograph of figure 6 shows a microstructure consisting of many overlapping semi-circular lines. These lines are the boundary of melt pools produced by melting of powders during SLM. Average size of the melt pools obtained is about 100 μm. Decreasing the melt pool size will increase the strength of an SLM product. This could be accomplished by optimizing various experimental parameters such as laser power, scan speed, scan spacing and layer thickness. The right side micrograph of the figure is a microstructure of the melt pool taken at higher magnification. There are two dark parallel lines at the center of the micrograph. These lines show the boundary between two arbitrary melt pools. The rest of the structures show various dendritic grains within the melt pools. The formation of dendrites and their implication are the same as that mentioned earlier (for the case of Concept stainless steel).

2.1.3 EOS Stainless Steel

This powder is a proprietary stainless steel powder (Cr-15-17.5%, Ni- 3-5%, Cu- 3-5%, Mn- max 1%, Si- max 1%, Mo- max 0.5%, Nb- 0.15-0.45%, C- max 0.07%, Fe-rest) of average size 25 μm named as EOS StainlessSteel 17-4

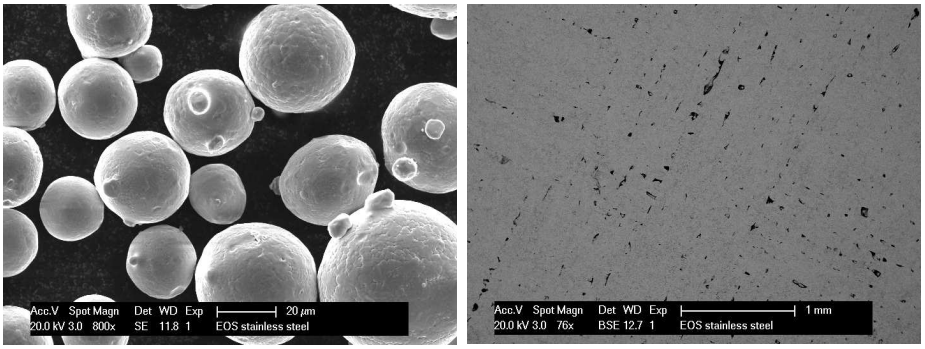

Fig. 7. Micrographs of powder and part of EOS stainless steel

supplied by EOS GmbH and is developed for EOS' own machine EOSINT M 270.

It has been processed on the Concept Laser machine using the following parameters: Laser Power- 95 W, Scanning Speed- 350 mm/s, Scan Spacing- 140 μm, Layer Thickness- 30 μm, Scanning Strategy- chess board islands. The processed part is subsequently treated in an oven for 1 hour at 650°C for removing of residual stresses. The density obtained is 98% and the hardness is 19 HRC.

Figure 7 shows micrographs of the powder and the part in the case of EOS stainless steel material. The powder particles are all completely spherical which was not the case for Concept Laser powders (see Figures 2 and 5) . The microstructure of the parts show the presence of pores (dark spots) in lines. A bunch of parallel lines of pores are perpendicular to the other bunches showing the intersection of two chess boards islands. The presence of pores in scan lines (direct laser-powder interaction lines) confirms the earlier finding that the scan lines are the main source of pore formations. The pores are more prominent in the micrograph (see the left side micrograph of Figure 8) of the EOS stainless steel material which has not been processed in oven (henceforth termed as un-annealed EOS stainless steel). This shows that oven treatment has tried to decrease the size the pores.

Figure 9 shows the etched microstructure of annealed samples at higher magnification. The micrograph on the left shows various dark lines which are grain boundaries. These grain shapes unlike the grain shapes found earlier for other materials and EOS stainless steel (see the right side micrograph of Figure 8) look like approaching circles. This could be the result of the stress-relieving heat treatment which helped diffusion to take place and reshaped the existing grains. The right side micrograph shows the same microstructure at still higher magnification. The dendritic structure as obtained for other SLM materials is also present here, be it that the dendritic structure is much finer in this case.

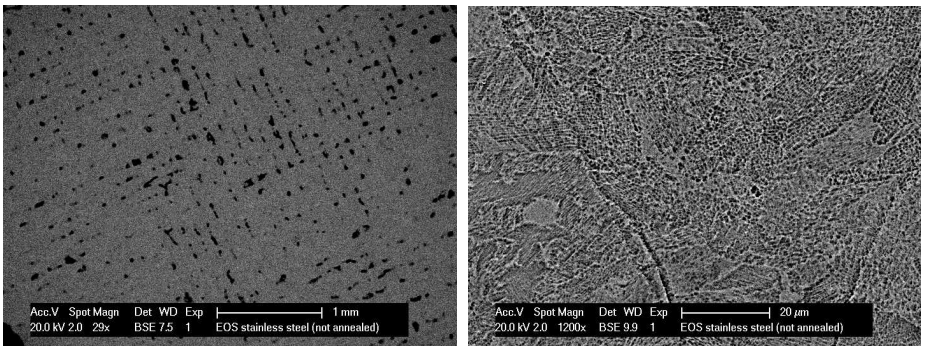

Fig. 8. Micrographs of part of un-annealed EOS stainless steel

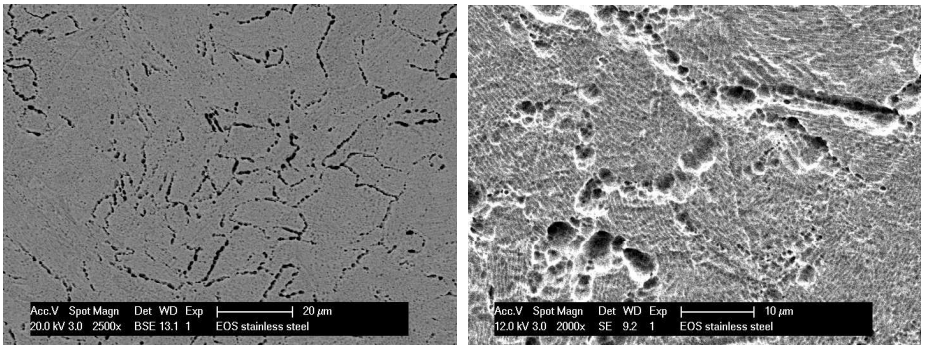

Fig. 9. Micrographs of annealed EOS stainless steel at higher magnifications

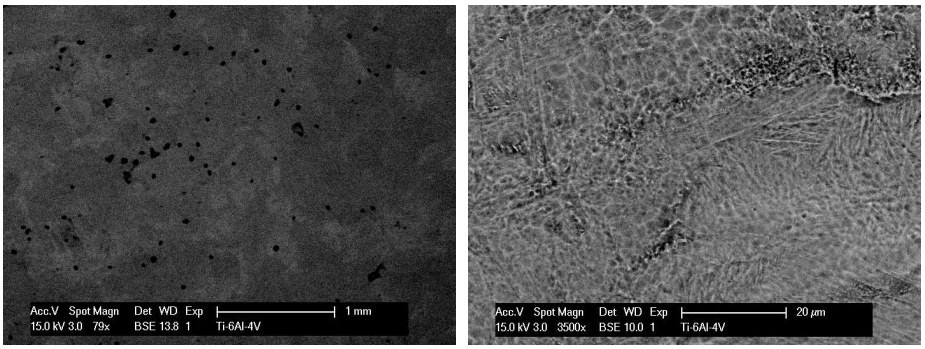

Fig. 10. Micrographs of part of Ti-6Al-4V

2.1.4 Ti-6Al-4V and Co-Cr-Mo

The Ti-6Al-4V powder is obtained from Concept Laser GmbH and its trade name is CL 40Ti. It is of size 25-45 μm (average size- 35 μm) and is spherical in shape. Co-Cr-Mo is locally made using an induction melting gas atomization process and is of average size of 50 μm. Its composition is Co- 63%, Cr- 29.53%, Mo- 5%, Si- 1%, Mn- 0.5%, Fe- 0.5%, N- 0.3%, C- 0.17%. These materials are widely used in medical applications because of their excellent bio-compatibility.

Both powders have been processed on the Concept Laser machine using the following parameters: Laser Power- 95, 95 W, Layer Thickness- 30, 40 μm,

Scan Speed- 125, 200 mm/s, Scan Spacing- 130, 140 μm for Ti-6Al-4V and Co-Cr-Mo respectively. SLM parts thus obtained gave more than 99% density. Details of other characteristics can be found elsewhere [5].

Micrographs of Ti-6Al-4V are given in Figure 10. The left side micrograph of Figure 10 shows dark spots on the microstructure which are pores. A smaller number of pores in comparison to that of other SLM materials gives the evidence of higher density percentage of Ti-6Al-4V. At higher magnification, smaller grains of about 5μm, besides various phases of Ti-6Al-4V are seen in the right side micrograph of Figure 10.

2.2 SLS Materials and Processing

2.2.1 LaserForm

LaserForm ST- 100 is a polymer coated steel powder of average size 100 μm supplied by 3D Systems to be processed on DTM SLS Sinterstations. The steel powder contains Cr- 12-14%, Mn- 1%, Si- 1% and the rest iron. These steel grains are coated with a proprietary organic binders containing less than 0.1% formaldehyde and phenol. The powders have been processed using the following fabrication parameters: Laser Power- 12.5 W, Layer Thickness- 80 μm, Scan Spacing- 80 μm, Scan Speed- 1680 mm/sec and Spot Size- 600 μm.

The laser-sintered parts were debinded (polymer burn out) and infiltrated with bronze in an oven. Oven cycle used for infiltrating consists of three steps [8]: debinding of polymers at 450 to 650°C, sintering of remaining steel after polymer burn-out at about 700°C, and infiltration of part at approximately 1050°C. The final composition of the part is about 60 % steel and 40 % bronze.

The final parts have characteristics similar to P20 steel: hardness of 83.4 HRB, density 7.7 g/cm^3, Young's Modulus 137 GPa, Tensile yield strength 305 MPa, Compressive yield strength 317 MPa and ultimate tensile strength 510 MPa.

2.2.2 DirectSteel

DirectSteel 20 V1 is a powder of average size 20 μm supplied by the company EOS. It consists of Fe 60%, Ni 31% and Cu_3P 9%, C 0.08%. Parts tested here were manufactured using a skin and core scanning strategy by a laser sintering machine, EOSint M 250 Xtended, equipped with a CO_2 laser. In this strategy, the outer skin of the parts is processed with higher laser energy density to make the surface denser and stronger in comparison to the core. Fabrication parameters used are: Layer Thickness 20 μm (skin) and 40 μm (core), Laser Power 20 W, Spot Size 300 μm, Hatching Distance 200 μm (skin) and 300 μm

(core), Scan Speed- 255 mm/s (skin) and 111 mm/s (core).

The stated properties of the laser sintered materials are: density (skin) 7-7.6 g/cm^2, density (core) 6-6.3 g/cm^2, hardness 89.6 HRB, Young's Modulus 130 GPa and Ultimate tensile strength 600 MPa [9].

2.3 Fretting Wear Test

Fretting is a wear phenomenon occurring when two contacting solids are subjected to a relative, oscillatory, tangential motion of small displacement amplitude [10]. Fretting can be applied by (1) keeping the counterbody fixed and linearly vibrating the specimen, (2) keeping the specimen fixed and linearly vibrating the counterbody. In the present case, type 1 has been adopted. The specimen is mounted on a translation table which can be oscillated by a stepping motor. The displacement of the specimen is measured by an inductive displacement transducer and the friction force is measured with a piezoelectric transducer. The friction coefficient and total dissipated energy are calculated from the on-line measured tangential force [11].

Fretting tests were performed to evaluate the wear characteristics of the SLS/SLM materials. The amplitude and frequency of oscillation as well as environmental conditions were kept constant for all experiments. Experimental parameters were selected in such a way that all tests could be executed under elastic contact conditions. A chrome steel ball of 30 mm was selected as counterbody. The parameters for the tests were as follows: Applied load- 2, 4, 6 N, Sliding distance (amplitude)- 200 μm, Frequency- 10 Hz, No. of cycles- 10,000, Temperature- 25°C and Humidity- 52%.

3 Results and Discussions

The Coefficient of Friction (COF) and wear volumes were determined for each material. COFs were found to be between 0.5 and 0.8 for all samples and showed a decrease with an increase in applied loads. Wear volumes obtained for all samples are given in table 2. Wear volumes for SLS materials such as LaserForm and DirectSteel are also given for comparison. Wear volumes of milled tool steel are also added in the table for comparing with the wear resistance of SLS/SLM material with that of a conventional manufactured material. The composition of the tool steel in percentage is C- 0.40, Cr- 1.90, Mo- 0.20, Mn- 1.5, S- 0.07, Si- 0.40, Fe- bal and its hardness is 31.6 HRC.

Table 2 shows that the wear of Concept tool steel is maximum and much more

Material	Applied Load (N)	Wear Vol. ($10^3 \mu m^3$)
Concept Stainless Steel	2	15
	6	51
Concept Tool Steel	2	198
	6	462
EOS Stainless Steel	2	39
	6	66
Ti-6Al-4V	2	7362
	6	9337
Co-Cr-Mo	2	1474
	6	2252
LaserForm	2	10.7
	4	29.6
DirectSteel	2	53.9
	4	83
Milled tool steel	2	360
	4	420
	6	586
tool steel (UHB 11)	6	5442
Hardened tool steel (UHB 11)	6	3899

Table 2
Wear volumes obtained after fretting tests

than other materials. This was unexpected as tool steel is supposed to furnish better wear resistance than other steels. Wear of EOS stainless steel is more than Concept stainless steel. It shows that wear resistance of steel-based SLM materials is not dependant on their hardness and decreases with an increase in hardness.

Bio-materials Ti-6Al-4V and Co-Cr-Mo give the least wear-resistance and are not suitable for any wear applications. The performance of SLS material LaserForm is unexpectedly better than both SLM stainless steels. It could be due to the presence of a low-friction element (copper) in LaserForm which helped increase its wear resistant. It shows that the composition of the material is more important than the type of processing for developing a wear-resistant material.

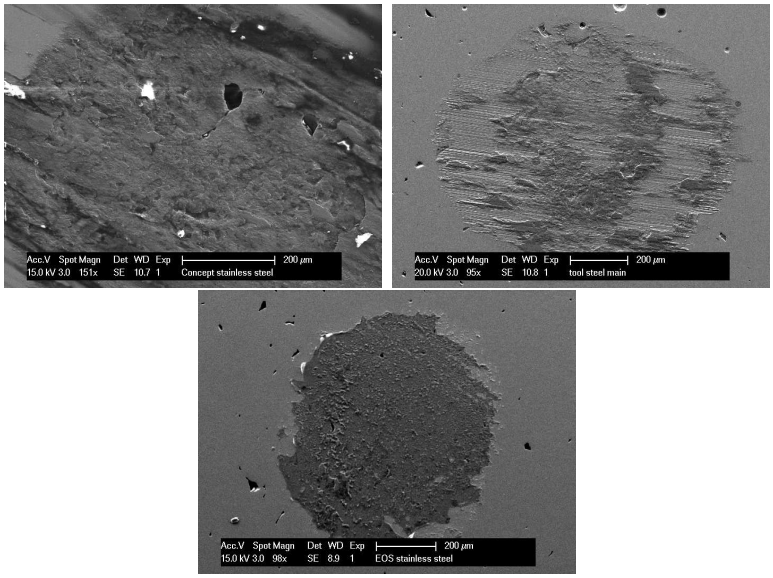

Fig. 11. Fretting wear zones of Concept stainless steel, Concept tool steel and EOS stainless steel respectively

Another conventionally produced tool steel UHB 11 (C 0.5, Si 0.3, Mn 0.6, S 0.04, Fe rest) (hardened at 850°C, 30 min., quenching medium water) was also used for the wear testing under the same condition to observe the effect of hardening on the wear performance. It was found that hardening increases its wear resistance almost twice but even then, the wear resistance is far less than the SLS/SLM materials. Its wear resistance is also very different from another tool steel used, showing again that composition significantly influences the wear behaviour of materials.

All iron-based SLS/SLM materials give higher wear resistance than conventionally produced milled tool steel showing that SLS/SLM techniques are capable of producing products with superior properties and can be efficiently used for rapid tooling.

Fretting wear zones of Concept stainless steel, Concept tool steel and EOS stainless steel are given in figure 11. These have been obtained after cleaning the samples in an ultrasonic bath after fretting tests. Micrographs show that thin films have been formed on fretting zones of the stainless steel samples while agglomerated debris are shown in the wear zone of tool steel. These films protect the surface from further wear and are responsible for smaller wear volumes in comparison to that of tool steel. Micrographs of tool steel wear zones shows scratching lines stating that abrasive wear is the main cause for its fretting degradation.

Stainless steels are electro etched using 10% oxalic acid to reveal the microstructure of their wear zones. Figure 12 shows the micrographs obtained for Concept stainless steel. The micrograph shows that the wear surface is full

of circular depressions. These plastic depressions are the result of trapping of hard wear debris (from chrome steel) between fretting surfaces. It demonstrates that the main mechanism of wear of stainless steel is the excavation of surface by wear debris.

4 Conclusion

In all cases pore-free SLM parts have not been obtained showing that there is a need for improving the powders which could be processed by more than one machine. The porosity of the part could not be removed by heat treatment as shown for EOS stainless steel parts. Infiltration is also not an option to decrease the porosity of SLM products. Other techniques such as HIPing could possibly be exercised for obtaining complete pore-free products.

The microstructure produced in the case of SLM is better than casted iron furnishing higher strength. It could be possible to refine the microstructures by increasing the temperature gradients which is possible by increasing the laser power and scan speed.

SLM stainless steel gives better wear resistance than SLM tool steel. The wear resistance of tool steel could be improved by incorporating low friction element in its composition. COF for all materials are high which shows that an extensive research needs to be done for decreasing the COF.

The materials tested were not 100% dense. Better wear resistance could probably be obtained for fully dense materials which could be achieved by careful optimization of SLM parameters.

A dedicated SLS material (i.e. LaserForm) has given better wear resistance than SLM stainless steel and tool steel. It shows that preferring SLM over SLS for Rapid Tooling is not necessarily the best choice.

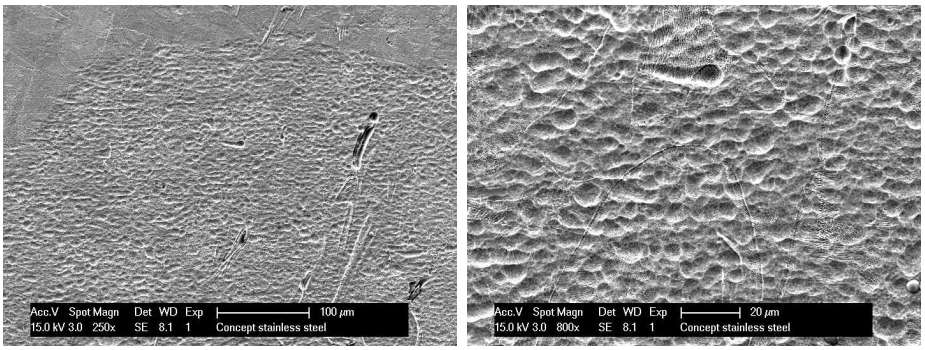

Fig. 12. Micrographs of etched fretting wear zone of Concept stainless steel

Wear volume of conventionally produced tool steel is very high in comparison to all other materials showing that the SLS/SLM technique is capable of offering excellent surface properties.

Acknowledgements

The author acknowledges K. U. Leuven, Belgium for granting him experimental facilities to carry out the research work.

References

[1] J. P. Kruth, G. Levy, F. Klocke, and T. Childs. Consolidation phenomena in laser and powder-bed based layer manufacturing. *CIRP Annals, vol 56, No. 2, pp. 730-759*, 2007.

[2] M. Rombouts. *Selective Laser Sintering/Melting of iron-based powders.* PhD thesis, Katholieke Universiteit Leuven, 2006.

[3] F. Petzoldt, H. Pohl, A. Simchi, and B. Alcantara. Advanced steel powder for direct metal laser sintering. *Proceedings of EuroPM2005 Conference 3, pp. 35-40*, 2005.

[4] T. B. Sercombe and G. B. Schaffer. The production of aluminium SLS prototypes via infiltration. *Proceedings of the VRAP 2003, Leiria, Portugal, pp. 297-301*, 2003.

[5] B. Vandenbroucke and J.-P. Kruth. Selective laser melting of biocompatible metals for rapid manufacturing of medical parts. *Rapid Prototyping Journal, vol. 13, No. 4, pp. 196-203*, 2007.

[6] J.-P. Kruth, L. Froyen, J. Van Vaerenbergh, P. Mercelis, M. Rombouts, and B. Lauwers. Selective laser melting of iron based powder. *Journal of Materials Processing Technology*, 149(1 - 3):616 – 622, 2004.

[7] S. Kumar. *SLS of Iron-based Powders and SLS/SLM for Rapid Tooling.* PhD thesis, K. U. Leuven, 2008.

[8] S. Kumar and J. P. Kruth. Effect of bronze infiltration on laser sintered metallic parts. *Materials and Design, vol. 28, issue 2, pp. 400-407*, 2007.

[9] S. Kumar, J. P. Kruth, and J. Van Humbeeck. Sliding wear behaviour of laser sintered moulds. *2nd International Conference on Polymers and Moulds Innovations, Ghent,Belgium, April 19-20*, 2007.

[10] H. Mohrbacher, J.-P. Celis, and J. R. Roos. Laboratory testing of displacement and load induced fretting. *Tribology International, vol 28, No 5, pp. 269-278*, 1995.

[11] B. Basu, J. Vleugels, and O. Van Der Biest. Microstructure-toughness-wear relationship of tetragonal zirconia ceramics. *Journal of the Europian Ceramic Society, vol. 24 pp. 2031-2040*, 2004.